RESEARCH ARTICLE

A Single-Photodiode Framework for the Co-Detection of Hybrid Digital and Analog Radio-Over-Fiber Signals

GUO HAO THNG[1], (Member, IEEE), AND SAID MIKKI[1,2], (Member, IEEE)

[1]Zhejiang University-University of Illinois Urbana-Champaign (ZJU-UIUC) Institute, Zhejiang University, International Campus, Haining, Zhejiang 314400, China
[2]Department of Electrical and Computer Engineering, University of Illinois Urbana-Champaign, Urbana, IL 61820, USA

Corresponding author: Said Mikki (smikki@illinois.edu)

ABSTRACT The continuous advancement of wireless mobile communication necessitates an increase in the allocated frequency bands for each generation. Consequently, higher frequency photodiodes are required in analog radio-over-fiber (ARoF) fronthaul solutions. However, the limited available bandwidth in the wireless domain poses challenges to efficiently utilize the capacity of these photodiodes. To overcome this obstacle, this paper explores the utilization of a single-photodiode base station configuration to enable hybrid digital radio-over-fiber (DRoF) and ARoF transmission. Furthermore, it proposes a straightforward signal processing approach to effectively separate the distinct analog and digital radio-over-fiber signals. To evaluate the feasibility of the proposed signal processing method, software simulations were conducted. The initial findings indicate that the combination of a single-photodiode base station configuration and the suggested signal processing approach holds promise for hybrid digital and analog radio-over-fiber systems. It demonstrates the potential to minimize the number of required photodiodes, thus improving efficiency in the context of limited available bandwidth.

INDEX TERMS Analog radio-over-fiber, centralized radio access network, digital radio over fiber.

I. INTRODUCTION

Within the overall framework of centralized radio access networks (CRAN), two competing technologies exist: digital radio-over-fiber (DRoF) and analog radio-over-fiber (ARoF) [1]. The fundamental disparity between these two RoF technologies lies in the nature of the signal conveyed over the fiber link connecting the central office and the base station. Each technology possesses its distinct strengths and weaknesses. DRoF involves the digitization of radio signals prior to optical modulation, typically employing amplitude modulation (AM) to modulate the optical carrier. In contrast, ARoF directly modulates the optical carrier with the radio signals. Consequently, the optical transmitter utilized for ARoF signal transmission exhibits comparatively higher complexity when compared to DRoF. Nonetheless, the

The associate editor coordinating the review of this manuscript and approving it for publication was Mohamed M. A. Moustafa.

base station configuration for an ARoF link can be further streamlined due to the fact that the electrical signal obtained after photodiode heterodyne detection is already in the form of an RF waveform. In contrast, in the case of DRoF, the amplitude-modulated signal is relatively less prone to non-linear impairments stemming from the optical transmission link, as compared to ARoF signals [2]. However, the inherent nature of digitizing radio signals in Common Radio Public Interface (CRPI)-based digital DRoF schemes introduces a significant number of quantization bits and entails baseband signal transmission. Consequently, these DRoF schemes are not inherently spectrally efficient [3]. As a result, while there are on going research efforts in mitigating the weaknesses of each technology [4], the choice between DRoF and ARoF deployment depends on the specific circumstances and criteria set forth by the service provider. In certain scenarios, ARoF may be deemed more suitable, while in others, DRoF may be the preferred option. Thus, it is highly

probable that both technologies will coexist within an access network.

The co-transport of baseband signals and RF signals through fiber for hybrid optical access networks has gained significant attention in the research community. A hybrid optical access network has been proposed, which employs hybrid multiplexing of multiband wavelength-interleaved signals within an integrated dense wavelength division multiplexing (DWDM) access network [5]. However, the previously demonstrated implementation utilizes multiple optical sources and modulators to modulate optical carriers for different optical access network technologies [5]. To address this complexity, a simplified optical transmitter configuration has been proposed and demonstrated [6], [7], [8]. This configuration utilizes a single dual-arm Mach-Zehnder modulator to enable simultaneous modulation of both baseband and RF signals [6], [7], [8]. This approach offers a more streamlined solution for hybrid optical access networks, reducing the need for multiple optical sources and modulators. These advancements in optical transmission technologies pave the way for more efficient and effective co-transport of baseband and RF signals in hybrid optical access networks, ultimately enhancing the overall performance and scalability of such networks. The utilization of polarization division multiplexing (PDM) schemes offers the potential for more efficient bandwidth utilization in optical communication systems. However, it is important to note that the additional complexity associated with polarization division demultiplexing introduces challenges in the link architecture [9]. In order to further enhance the optical spectral efficiency, a study presented in [10] explores the modulation of the ARoF signal within the spectrum of the DRoF signal. By extracting the ARoF signal from the combined signal through subtraction, exploiting the distinct characteristics of DRoF and ARoF signals, improved spectral efficiency can be achieved [10]. Similar studies has also been carried out for hybrid fixed-mobile networks, where the wireless signals are modulated at the null point of the baseband signal for passive optical network (PON) [11], [12], [13]. Nevertheless, it is worth noting that the focus of the aforementioned research studies primarily revolves around the generation of optical tones to facilitate signal transmission in hybrid optical access technologies. These investigations emphasize the development and optimization of various signal generation techniques within the context of hybrid optical access systems.

In the context of an ARoF link, the utilization of a high-speed photodiode may face limitations in fully exploiting the photocurrent output due to the restricted bandwidth available for wireless transmission. This limitation becomes more pronounced as higher frequency bands are being proposed for the use of 6G and beyond wireless communication [14]. To illustrate this point, let's consider the currently deployed 5G frequency band as an example. If ARoF is employed to support the 5G band n260, which has a bandwidth of 3 GHz and operates within the frequency range

of 37 GHz to 40 GHz, the high-speed photodiode utilized must have a 3-dB bandwidth of 40 GHz, even though the wireless signal occupies less than 10 percent of the total available bandwidth. This scenario highlights the inefficiency of using a high-speed photodiode in terms of bandwidth utilization. A significant portion of the available bandwidth remains unused, leading to a suboptimal utilization of the photodiode's capabilities. As higher frequency bands are being considered for future wireless communication systems, it becomes crucial to explore alternative approaches that can better utilize the available bandwidth and maximize the performance of the ARoF link. To address this challenge, this paper investigates the feasibility of employing a single-photodiode to enable the detection of both ARoF and DRoF signals within a single base station or remote antenna site. We propose a straightforward signal processing approach within a single-photodiode framework for the co-detection of hybrid digital and analog RoF signals. Previous studies, such as [11], [12], [13], have indeed demonstrated the use of a single photodiode for the co-detection of various signals in specific contexts. For example, in the context of PON, some studies [12], [13] have explored the co-detection of baseband pulse amplitude modulated (PAM) signals, while in wireless communication networks, other studies [11], [12] have investigated the co-detection of non-orthogonal multiple access with carrierless amplitude and phase (CAP) or orthogonal frequency division multiplexing (OFDM) based modulated signals. However, a comprehensive investigation of the usage of a single photodiode for co-detection across different signal types and network contexts has not been conducted. While previous studies have provided valuable insights and demonstrated the feasibility of co-detection with specific signal types, a comprehensive exploration is needed to assess the performance, limitations, and potential benefits of using a single photodiode for co-detection across a broader range of signals and network scenarios. Such a comprehensive investigation would contribute to a deeper understanding of the capabilities and challenges associated with the use of a single photodiode for co-detection, enabling more informed design and optimization of photonic systems for various communication networks. Furthermore, in [15], the utilization of CAP modulation for the DRoF link was demonstrated, enabling the use of a single-photodiode to support the co-detection of both ARoF and DRoF signals.

The demonstration conducted in [15] effectively mitigates the issue of baseband signal-to-signal beating interference by shifting the CAP signal, after photodiode detection, to a higher frequency range. This necessitates the use of filters to modulate the CAP signal at the elevated frequency. However, it is important to consider that as the bandwidth of the beating signal at baseband, resulting from the homodyning of both DRoF and ARoF signals, increases, the CAP signal may need to be further shifted to even higher frequencies. This can present challenges, particularly in the face of escalating demands for higher

data rates. In contrast, the proposed single-photodiode signal processing framework given in this paper offers greater flexibility by accommodating various modulation formats, rather than being limited solely to CAP modulated signals for DRoF links. This capability allows for the exploration of alternative modulation schemes that may better suit specific requirements, including those driven by the need for higher data rates. By enabling the use of different modulation formats, the proposed framework expands the design space and offers potential avenues for addressing the growing demand for increased data transmission capabilities.

II. THEORETICAL ANALYSIS OF THE PROPOSED SINGLE-PHOTODIODE FRAMEWORK

In a hybrid DRoF and ARoF system employing a single-photodiode, it is crucial to ensure the separability of the resultant signals after heterodyned detection for each individual ARoF and DRoF link. The modulation format utilized for the ARoF signal plays a significant role in determining the separability of the heterodyned signals. After photodiode heterodyne detection, the DRoF signal typically resides at the baseband frequency, while the ARoF signal generates two components: one at the desired frequency for wireless transmission and another at baseband, corresponding to the squared amplitude of the ARoF signal. The baseband component acts as additive noise, which, when combined with the DRoF signal, can degrade performance or even corrupt the DRoF signal, depending on the signal power. To address this challenge, we propose a simple signal processing approach in this paper. This approach involves extracting the squared amplitude of the ARoF signal and subtracting it from the baseband DRoF signal. The proposed signal processing method can be implemented in the analog domain using components such as a square-law detector, low-pass filter, attenuator, and a differential amplifier, thereby eliminating the need for a digital signal processor (DSP). However, it is also possible to implement the approach using a DSP if desired. By adopting this straightforward signal processing technique, the hybrid DRoF and ARoF system can effectively separate the desired signals from the baseband noise, enhancing the overall system performance.

We first start by providing a brief theoretical analysis which is based on the following assumptions. First, there are three optical tones that are present at the base station before photodiode detection, and the optical tones are assumed to be generated using the optical transmitter shown in Figure 1. Second, it is assumed that the received optical signals are represented by the following equation

$$E_r(t) = e^{j\{2\pi f_1 t + \phi_1(t)\}} + A_d(t)e^{j\{2\pi f_2 t + \phi_2(t)\}}$$
$$+ A_a(t)e^{j\{2\pi f_1 t + 2\pi f_{RF} t + \phi_a(t) + \phi_1(t)\}}, \quad (1)$$

where $A_d(t)$ is the amplitude modulated DRoF signal, f_{RF} is the RF carrier frequency for the ARoF signal, f_1 and f_2 are
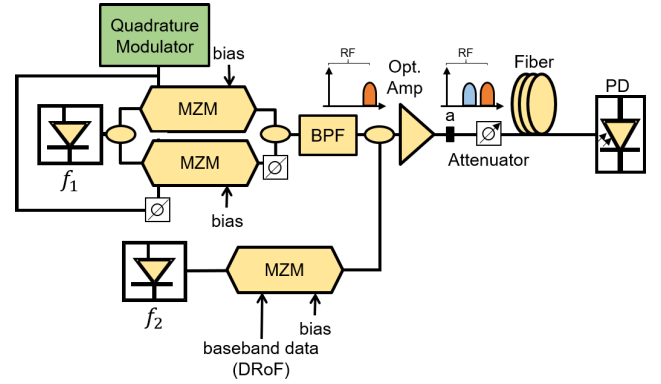

FIGURE 1. An example of an optical transmitter configuration for co-transmission of hybrid ARoF/DRoF signals, where MZM refers to Mach-Zehnder modulator.

the operating frequency of the optical sources, and $\phi_1(t)$ and $\phi_2(t)$ are the phase fluctuation of the optical sources. The amplitude and phase of ARoF signal is represented by $A_a(t)$ and $\phi_a(t)$.

When the signal (represented by (1)) is detected by the photodiode, the photocurrent output after photodiode detection would be

$$I_{ap}(t) = \Re\left[E_r(t) \times E_r(t)^*\right]$$

$$= \Re\Big[1 + A_d^2(t) + A_d(t)e^{j\{2\pi(f_1-f_2)t+\phi_1(t)-\phi_2(t)\}}$$
$$+ A_a(t)e^{j\{-2\pi f_{RF}t-\phi_a(t)\}}$$
$$+ A_d(t)e^{-j\{2\pi(f_1-f_2)t+\phi_1(t)-\phi_2(t)\}}$$
$$+ A_d(t)A_a(t)e^{j\{2\pi(f_2-f_1-f_{RF})t-\phi_a(t)+\phi_2(t)-\phi_1(t)\}}$$
$$+ A_d(t)A_a(t)e^{j\{2\pi(f_1+f_{RF}-f_2)t+\phi_a(t)-\phi_2(t)+\phi_1(t)\}}$$
$$+ A_a(t)e^{j\{2\pi f_{RF}t+\phi_a(t)\}} + A_a^2(t)\Big], \quad (2)$$

where $E_r^*(t)$ is the conjugate of $E_r(t)$. Simplifying (2), we obtain

$$I_{ap}(t) = \Re\Big[1 + A_d^2(t) + 2A_a(t)\cos\{2\pi f_{RF}t + \phi_a(t)\}$$
$$+ 2A_{ad}(t)\cos\{2\pi(\Delta f - f_{RF})t - \phi_a(t) + \Delta\phi(t)\}$$
$$+ 2A_d(t)\cos\{2\pi\Delta f t + \Delta\phi(t)\} + A_a^2(t)\Big]. \quad (3)$$

Here, $\Delta f := f_2 - f_1$, $\Delta\phi(t) := \phi_2(t) - \phi_1(t)$, $A_{ad}(t) := A_a(t) \times A_d(t)$. The constant $\Re$ is the responsivity of the photodiode. A lowpass filter is deployed to extract signals at baseband frequency, while a bandpass filter is used to extract the signal at f_{RF}. For simplicity, let $\Re = 1$ and assume that the deployed filters do not introduce any insertion loss.
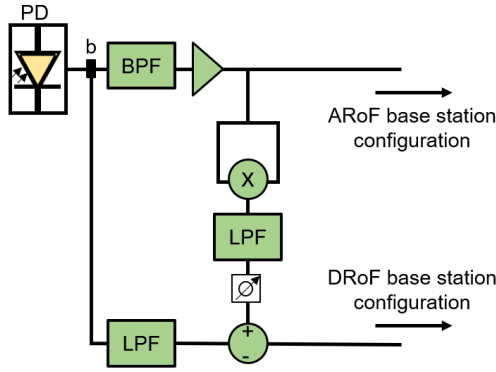
FIGURE 2. Proposed signal processing approach for single-photodiode (PD) base station configuration.

TABLE 1. Simulation parameters.

Parameters	Values
Bitrate	10 Gbps
Modulation	ARoF: QPSK, 16 QAM, DRoF: On-Off Keying
RF carrier	100 GHz
Optical Carrier	193.1 THz, 193.16 THz
Optical Power	Fiber Launch Power: $\{-1 \text{ dBm}, 1.8 \text{ dBm}\}$ Received Optical Power: $\{-6 \text{ dBm}, -3.2 \text{ dBm}\}$
Laser Linewidth	1 MHz
Optical Bandpass Filter	Bandwidth: 100 GHz (193.2 THz)
Optical Amplifier	Gain: 20 dBm, Noise Figure: 6 dBm
Fiber	Length: 25 km, Attenuation: 0.2 dB/km Dispersion: 16.75 ps/nm/km Polarization Mode Dispersion: $0.05 \text{ ps}/\sqrt{\text{km}}$
RF Amplifier	Gain: 50 dB, Noise Figure: 6 dBm
Bandpass Filter	BW: 10 GHz (100 GHz)
Lowpass Filter	BW: 10 GHz (DRoF), 5 GHz (ARoF)
DSP	Carrier Phase Estimation

In this case, the extracted signals can be expressed as follows:

$$I_b(t) = A_d^2(t) + A_a^2(t) + 1 \tag{4}$$

$$I_{RF}(t) = A_a(t)\cos\{2\pi f_{RF}t + \phi_a(t)\} \tag{5}$$

where $I_b(t)$ and $I_{RF}(t)$ represent the filtered signal at baseband and at RF respectively.

As indicated by (4) and (5), while the ARoF signal can be extracted using a bandpass filter, it is not feasible to isolate the DRoF signal solely through filtering due to the presence of the term $A_a^2(t)$, which contaminates the baseband signal. For a single-photodiode to enable simultaneous detection of ARoF and DRoF signals, the term $A_a^2(t)$, arising from the homodyning of the ARoF signal with its own conjugate, must satisfy one of the following conditions: either it remains constant, has significantly lower power than $A_d^2(t)$, or it must be completely eliminated to ensure the integrity of the DRoF signal. Hence, in the absence of signal processing, utilizing a single-photodiode configuration may only be viable when the modulated ARoF signal exhibits phase variation without amplitude changes, such as in phase shift keying (PSK) signals. However, in wireless communication networks, besides M-ary PSK signals, M-ary quadrature amplitude modulation (M-QAM) signals are also utilized, which can vary in both phase and amplitude. Therefore, we propose a signal processing approach, depicted in Figure 2, to eliminate $A_a^2(t)$ at the baseband. This ensures that the DRoF signal can be extracted with a relatively high level of signal integrity, enabling the utilization of a single-photodiode configuration to support hybrid ARoF and DRoF systems. The proposed signal processing method leverages the extracted ARoF signal to eliminate or significantly suppress the $A_a^2(t)$ term at the baseband. This can be achieved by obtaining the squared value of (5), which yields the $A_a^2(t)$ term:

$$I_{RF}^2(t) = \left[2A_a(t)\cos\{2\pi f_{RF}t + \phi_a(t)\}\right]^2$$
$$= 2A_a^2(t)\left[\cos\{4\pi f_{RF}t + 2\phi_a(t)\} + \cos\{0\}\right]$$
$$= 2A_a^2(t) + 2A_a^2(t)\cos\{4\pi f_{RF}t + 2\phi_a(t)\}. \tag{6}$$

The signal $A_a^2(t)$ can be obtained by applying a lowpass filter to $I_{RF}^2(t)$. This signal, $A_a^2(t)$, can then be utilized to remove or subtract the contribution of $A_a^2(t)$ from $I_b(t)$.

The configuration shown above may be used for phase-modulated ARoF signals and possible 4-QAM signals. Phase modulated signals vary only in phase while having a fixed amplitude. Hence, the lowpass filtered $I_{RF}^2(t)$ will only be a DC signal [8], [16]. When the ARoF signal is phase modulated, the lowpass filtered photocurrent after photodiode detection can be represented as follows:

$$I_b(t) = A_d^2(t) + 2, \tag{7}$$

while the low pass filtered and attenuated $I_{RF}^2(t)$ will be

$$I_{RF\_LP}(t) = c, \tag{8}$$

where c is a constant. Subtracting the DC signal, $I_{RF\_LP}(t)$, from $I_b(t)$ will result in a DC offset that can be eliminated:

$$I_b(t) - I_{RF\_LP}(t) = A_d^2(t) + 2 - c. \tag{9}$$

Nevertheless, the presence of fiber and filters in the link introduces changes to the envelope of the phase-modulated ARoF signals, causing $A_a^2(t)$ to deviate from being a pure DC signal. Consequently, the degradation of the DRoF signal can occur even when utilizing phase modulation for ARoF. Therefore, in such scenarios, the signal processing structure depicted in Figure 2 could prove beneficial.

III. IMPLEMENTATION AND VERIFICATION
The proposed configuration utilizing a single photodiode, illustrated in Figure 2, is simulated in Optisystem 20 software using the parameters summarized in Table 1. The transmitter employed is similar to the one depicted in Figure 1, with its frequency spectrum shown in Figure 3. The performance of this configuration is assessed for ARoF signal transmission employing both phase-modulated signals (QPSK) and phase-and-modulated signals (16-QAM). To ensure that any improvements observed in the proposed signal processing
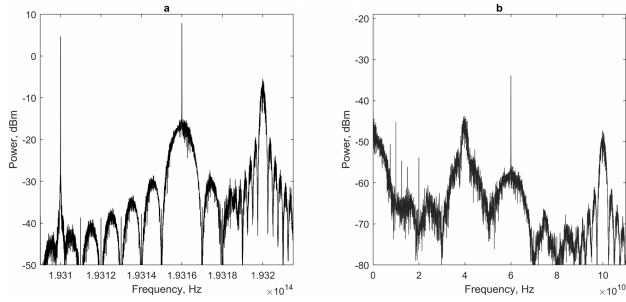
FIGURE 3. Optical spectrum at point a of **Figure 1** and RF spectrum at point b of **Figure 2**.

FIGURE 4. Estimated error rate of the ARoF signal with QPSK modulation, and DRoF signal with or without the proposed signal processing approach.

approach are solely attributed to its ability to mitigate the impairment caused by co-detection of hybrid digital and analog RoF signals using a single photodiode, the optical signal transmitted through the fiber is not further attenuated using an optical attenuator. It is maintained at a relatively high level, which serves two purposes: firstly, to emphasize the severity of the impairment, and secondly, to demonstrate the effectiveness of the proposed approach in mitigating it (as highlighted in Table 1).

As discussed in section II, $A_a^2(t)$ is an unwanted additive noise. Therefore, the power of the ARoF signal will affect the performance of the received DRoF signal in a single-photodiode base station. Hence, the proposed single-photodiode configuration is evaluated by varying the power of the ARoF signal, with δP representing the optical power difference between the ARoF signal P_a and the DRoF signal P_d measured before the optical coupler, i.e., $\delta P :=$ $P_a - P_d$. When $P_a \approx P_d$, the fiber launch power is approximately 0 dBm, the change in fiber launch power and the optical receiving power, as shown in Table 1, is contributed by varying P_a, while P_d is fixed. In other words, the power of the optical source for the DRoF link is fixed throughout the simulation for different δP values, and hence the DRoF signal strength is maintained before fiber transmission and before photodiode detection. Therefore, any performance gain or degradation of the DRoF link is contributed by the increase or decrease in P_a. Link performance is evaluated using error rate obtained by using eye diagrams to estimate the bit error rate (BER) for DRoF signal and constellation diagram by finding the symbol error rate (SER) for ARoF signal using 2^{17} bit sequence length, averaged through 5 simulation runs.

Figure 4 depicts the performance of the proposed single-photodiode configuration when QPSK modulation is employed for ARoF. As depicted in the figure, the performance of the ARoF link demonstrates enhancement with the increment of δP. This increase in δP results from an elevation in P_a, subsequently leading to an improvement in the signal-to-noise ratio of the ARoF link. On the other hand, the results obtained reveal that the DRoF link performance is influenced by the additive noise introduced by the ARoF signal. Surprisingly, the performance of the DRoF link experiences a rapid deterioration as the power of the ARoF signal increases (as shown in the figure). According to
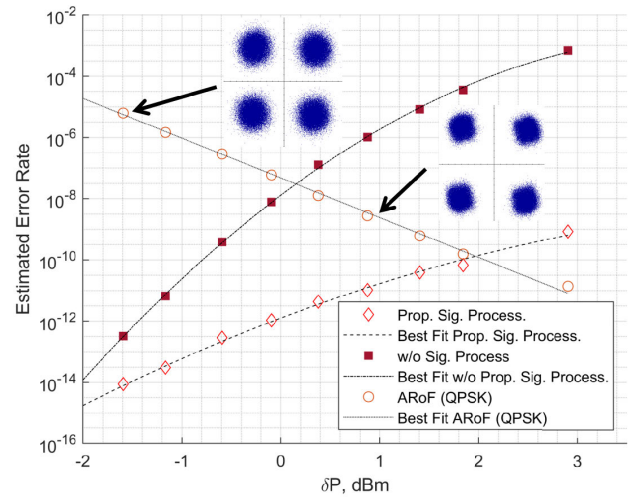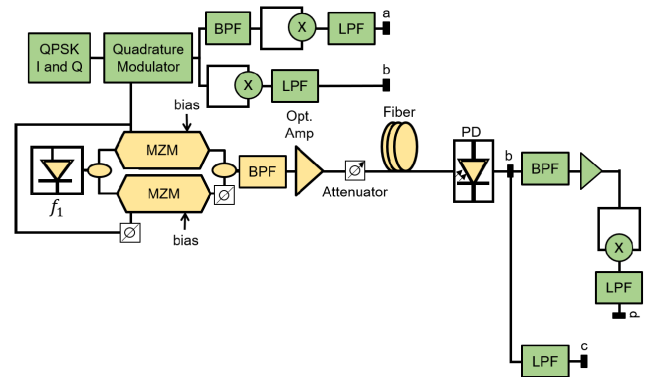

FIGURE 5. Test configuration for DRoF link performance degradation when phase modulated signal are used for ARoF link.

theoretical expectations, the squared amplitude of a phase-modulated signal, serving as a DC bias, should remain constant and have minimal impact on the DRoF link performance. However, contrary to these expectations, the results shown in Figure 4 indicate that an increase in ARoF signal power leads to the degradation of the DRoF signal. This degradation can be attributed to variations in the envelope of the ARoF signal caused by the presence of filters and impairments in the communication link. Such envelope fluctuations disrupt the constancy of the squared amplitude of the ARoF signal, transforming it from a constant DC signal to one that introduces distortion in the DRoF signal. To illustrate this effect, a similar configuration as depicted in Figure 5 is simulated using parameters listed in Table 1, highlighting the impact of filters and link impairments on the system. The resulting effects are presented in Figure 6. In the absence of filters, the squared amplitude of the phase-modulated QPSK signal remains relatively stable, as observed in Figure 6. However, when filters are employed, and due to impairments
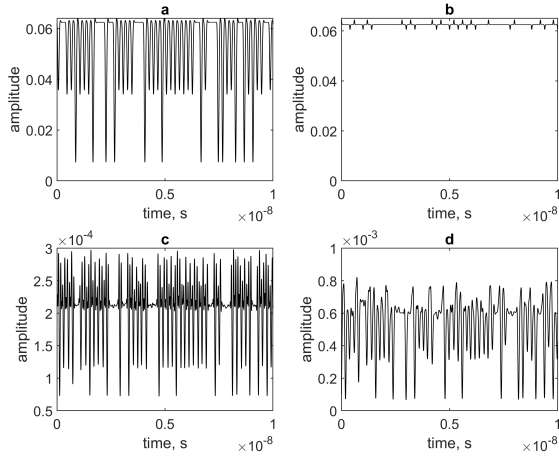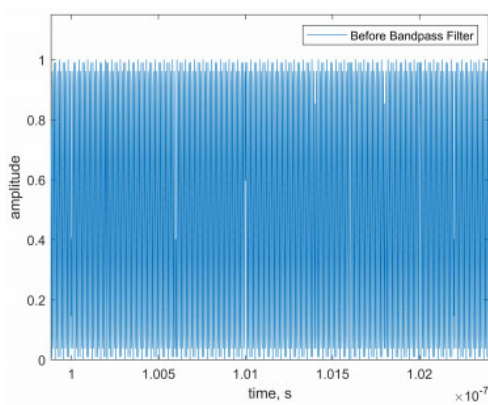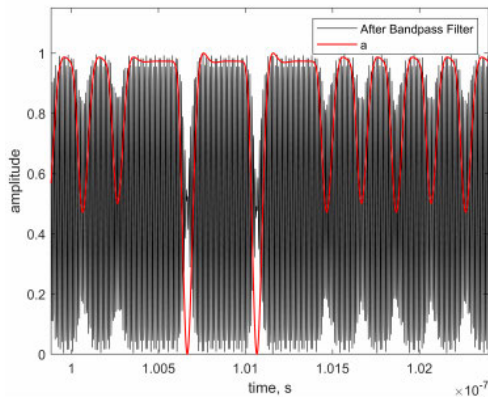
FIGURE 6. Time domain signal sampled at point (a) -(d) shown in Figure 5 for the first 10 ns.

(a) Before BPF

(b) After BPF

FIGURE 7. Normalized QPSK time domain signal sampled before and after the bandpass filter prior to point a of Figure 5.

introduced by the communication link, the low-pass filtered squared amplitude of the phase-modulated signal no longer remains constant. For instance, as illustrated in Figure 7, the bandpass filter modifies the signal's envelope, leading to observable amplitude fluctuations at point a in Figure 5.
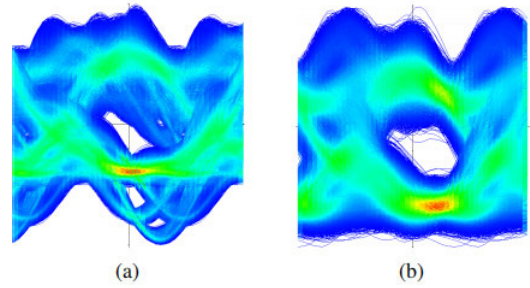

FIGURE 8. Eye diagram at $\delta P = 2.91$ dBm of the received DRoF signal (a) without the proposed signal processing approach and (b) with the proposed signal processing approach.
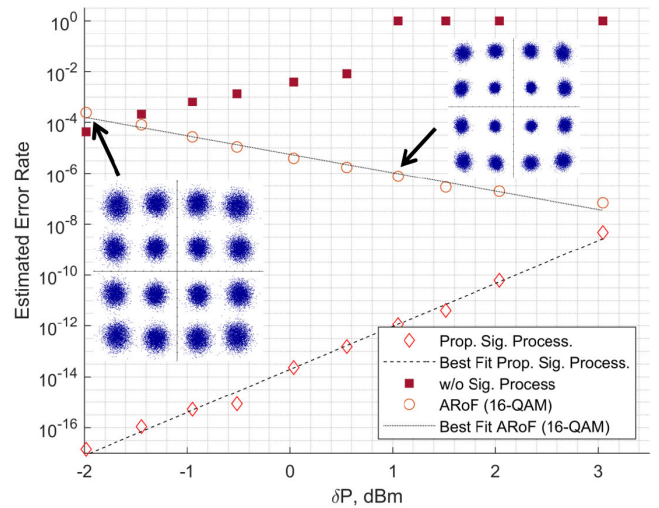

FIGURE 9. Estimated error rate of the ARoF signal with 16-QAM modulation, and DRoF signal with or without the proposed signal processing approach.

These amplitude fluctuations align with the variations in the QPSK signal's envelope. This phenomenon leads to performance degradation in the DRoF link. The results presented in Figure 4 indicate that the proposed signal processing approach effectively enhances the performance of the DRoF link by mitigating the effects of changes in the ARoF signal's envelope. Specifically, at $\delta P = -0.09$ dBm, the proposed signal processing approach significantly improves the DRoF link performance, reducing the estimated bit error rate (BER) from 10^{-8} to an impressive 10^{-12}. Furthermore, as depicted in Figure 8, when $\delta P = 2.91$ dBm, the proposed signal processing method notably enhances both the eye height and eye width in the DRoF signal's eye diagram. This improvement is clearly reflected in the obtained estimated error rate, as demonstrated in Figure 4. These results demonstrate the effectiveness and value of the proposed signal processing approach in mitigating the degradation caused by variations in the ARoF signal's envelope.

Conversely, when employing fluctuating amplitude and phase modulation schemes, such as 16-QAM, for the ARoF signal, the performance of the proposed single-photodiode configuration is depicted in Figure 9. Just like the ARoF link
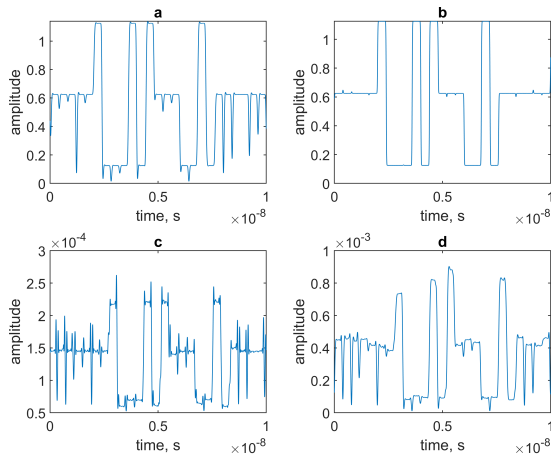
FIGURE 10. Sample time domain signal of $A_a^2(t)$ of the 16-QAM modulated ARoF signal at point (a)-(d) shown in Figure 5 for the first 10 ns.
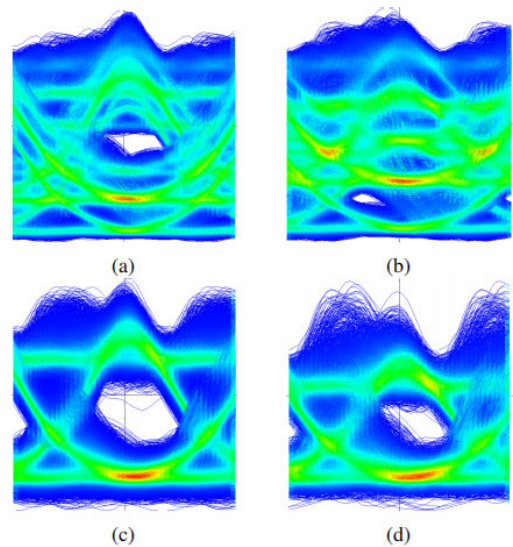

FIGURE 11. Eye diagram at $\delta P = 0.03$ dBm ((a) ,(c)) and $\delta P = 3.04$ dBm ((b),(d)) of the received DRoF signal with ((c)-(d)) and without ((a)-(b)) the proposed signal processing approach.

employing QPSK modulation, the error rate of the ARoF link utilizing 16-QAM modulated signals decreases as δP increases. This decrease in error rate is attributed to the improvement in the signal-to-noise ratio of the ARoF link due to the increasing δP. In addtion, the obtained results validate the analysis conducted in Section II and indicate that the proposed straightforward signal processing approach can enhance the detection accuracy of the DRoF signal in the presence of additive noise from $A_a^2(t)$. To visualize the additive noise $A_a^2(t)$, we conducted a simulation with a configuration similar to the one illustrated in Figure 5, using a 16-QAM signal and simulation parameters as outlined in Table 1. The resulting sampled time-domain signal of $A_a^2(t)$ is presented in Figure 10. As illustrated in Figure 9, the performance of the DRoF link deteriorates as the δP value increases, which corresponds to an increase in the power of the squared amplitude of the ARoF signal. In other words, a higher δP value leads to a lower signal-to-noise ratio in the DRoF link. These findings highlight the importance of the proposed signal processing approach in mitigating the adverse effects of increased noise levels and improving the performance of the DRoF link under such conditions. Conversely, the single-photodiode configuration, when equipped with the proposed signal processing approach, outperforms the configuration without signal processing by a significant margin. As shown in Figure 11, the eye diagram of the received DRoF signal has a wider opening when the proposed signal processing approach is used. Remarkably, at $\delta P = 0.03$ dBm, the proposed signal processing approach improves the performance of the DRoF link from an estimated bit error rate (BER) of 10^{-3} to an impressive 10^{-13} when utilizing a 16-QAM modulated ARoF signal. Comparing the results depicted in both Figure 4 and Figure 9, and the eye diagrams in Figure 8 and Figure 11, it is evident that while an increase in P_a, which corresponds to an increase in δP, degrades the performance of the DRoF link for both modulations, the presence of $A_a^2(t)$ has a more substantial impact on the DRoF

link performance when 16-QAM modulation is employed relative to QPSK modulation. As illustrated in Figure 4 and Figure 9, the performance of the DRoF link without the proposed signal processing is significantly lower when a 16-QAM modulated ARoF signal is used, compared to a QPSK modulated ARoF signal, for $\delta P \in \{-2, 3.5\}$. Moreover, the eye diagrams displayed in Figure 8 and Figure 11 strongly indicate that the proposed approach has the capability to effectively eliminate a significant portion of the amplitude noise introduced by $A_a^2(t)$. These results highlight the superior effectiveness of the proposed signal processing approach, particularly in mitigating the impact of $A_a^2(t)$ when utilizing 16-QAM modulation for the ARoF signal.

While the DRoF link is impacted by the $A_a^2(t)$ component of the ARoF signal, it's important to note that the $A_a^2(t)$ additive noise has distinct effects depending on the type of ARoF signal modulation, as evidenced in Figure 6 and Figure 10. As previously mentioned, the amplitude noise introduced when using a QPSK signal arises from variations in the QPSK signal's envelope. This additive amplitude noise results in "spikes" at different locations within the DRoF signal, as observed in the sampled time-domain signal in Figure 6 and the corresponding eye diagram shown in Figure 8. The variation in the envelope of the QPSK signal can be influenced by factors such as the signal's bit rate and the bandwidth of the filter employed. Conversely, in the case of the 16-QAM modulated signal, the $A_a^2(t)$ represents the squared amplitude of the 16-QAM signal. This squared amplitude disturbance affects the DRoF signal whenever there is a change in symbol amplitude, posing challenges for threshold detection as δP increases. This effect is clearly observable in the eye diagram of the DRoF signal presented in Figure 11 when no signal processing is applied. Similarly to the QPSK signal, the use of filters can also induce changes

in the envelope of the 16-QAM signal, resulting in the appearance of "spikes" at various points along the transmitted 16-QAM signal. However, as evidenced in Figure 10, the offset caused by fluctuations in symbol amplitude exhibits a larger amplitude compared to these "spikes," potentially leading to a more substantial impact on the DRoF signal. Increasing δP contributes to a reduction in the eye diagram's height at lower δP values and leads to eye closure when δP reaches higher levels. Upon observing the signal sampled at point b in the case of 16-QAM modulation, it becomes evident that there are three distinct amplitude levels present. This is because, given

$$[I \sin(2\pi ft) + Q \cos(2\pi ft)]^2, \qquad (10)$$

where $I, Q \in [-3, -1, 1, 3]$, at baseband, there will only be 3 amplitude levels at $\in [1, 5, 9]$.

The results presented in Figure 4 and Figure 9, along with the sampled time-domain signals depicted in Figure 6 and Figure 10, indicate that the proposed signal processing approach is unable to completely eliminate the additive noise contributed by the squared amplitude of the ARoF signal. In an ideal scenario, if the extracted $A_a^2(t)$ from the ARoF signal perfectly matches the $A_a^2(t)$ term present in the DRoF signal, the proposed signal processing approach can achieve flawless removal. This would lead to a reduced error rate for the DRoF link across all tested δP values and minimal or no performance degradation as δP increases. However, the sampled time-domain signals at points c and d in Figure 6 and Figure 10 are not identical, suggesting that the proposed signal processing approach, which involves extracting and subtracting $A_a^2(t)$ from the baseband DRoF signal, is not capable of entirely removing the effect of $A_a^2(t)$ on the baseband DRoF signal. Before extraction, the ARoF signal undergoes a different signal path with various types and numbers of filters, resulting in the extracted $A_a^2(t)$ being non-identical to the one present at baseband. As a result, the imperfect extraction of $A_a^2(t)$ from the ARoF signal leads to an imperfect removal of the $A_a^2(t)$ term from the DRoF signal. Although the obtained results suggest that the proposed signal processing approach can significantly suppress the effect of the additive noise contributed by $A_a^2(t)$, there remains a residual effect of $A_a^2(t)$ that distorts the DRoF signal, thereby causing degradation in link performance with increasing δP. Furthermore, when examining the estimated error rate of the ARoF link and increasing the number of bits per symbol, transitioning from 2-bits per symbol with QPSK modulation to 4-bits per symbol using 16-QAM modulation, it becomes apparent that the performance improvement with 16-QAM is less pronounced as δP increases (by augmenting P_a) compared to QPSK. This observation suggests that higher-order modulation schemes necessitate more power to attain equivalent performance levels in the ARoF link compared to lower-order modulation schemes. However, while higher-order modulations like 1024-QAM or even 4096-QAM are being proposed and demonstrated for wireless communication, the results presented in Figure 4 and Figure 9 indicate that achieving

acceptable performance for such high-order modulations would require δP values significantly exceeding 3 dBm, potentially impacting the performance of the DRoF link in the process.

Consequently, future research investigations should explore alternative methods to further enhance the performance of the proposed signal processing approach, enabling the effective co-detection of digital and analog RoF signals using a single photodiode. Several avenues can be explored in this regard. One possibility is to investigate the application of machine learning techniques to regenerate the distorted DRoF signal, leveraging the power of advanced algorithms to mitigate the residual effects of the additive noise. Additionally, it would be beneficial to explore other digital signal processing (DSP) equalization approaches in conjunction with the proposed signal processing technique. This combination may provide additional improvements in mitigating the distortions caused by the additive noise contributed by $A_a^2(t)$. Furthermore, a comprehensive study can be conducted to evaluate the performance of the proposed signal processing method when an additional ARoF signal is transmitted at the null-point of the DRoF signal. Investigating this scenario would provide valuable insights into the potential benefits and limitations of the proposed approach under different operating conditions. By exploring these avenues, researchers can further advance the performance and applicability of the proposed signal processing approach, ultimately enabling more efficient and robust co-detection of digital and analog RoF signals using a single photodiode.

IV. CONCLUSION

A signal processing approach has been proposed and demonstrated for a single-photodiode base station configuration that enables simultaneous hybrid DRoF and ARoF signal detection. The results obtained confirm that the single-photodiode configuration, when combined with the signal processing approach, enhances the performance of the DRoF link by effectively addressing the undesired squared amplitude component introduced by the homodyning of the ARoF signal at the baseband. This improvement in performance significantly enhances the versatility and capabilities of the single-photodiode base station configuration. Furthermore, the results also highlight that even when the ARoF signal is not transmitted at the null-point of the DRoF signal, the presence and strength of the ARoF signal still contribute to the degradation of the DRoF link performance. This finding underscores the importance of considering the impact of the ARoF signal strength on the overall performance of the DRoF link. Furthermore, the results obtained also indicate that enhancing the proposed signal processing approach may be imperative when employing higher-order modulation schemes for the ARoF link. This is due to the increased power requirements for achieving "error-free" wireless transmission with higher-order modulated signals, which could potentially impact the performance of the

DRoF link. Therefore, future research directions encompass exploring potential enhancements to the proposed signal processing approach and conducting further investigations to validate the findings of this study. It would be valuable to compare the performance of the proposed single-photodiode configuration with conventional multi-photodiode configurations, thus providing a comprehensive understanding of the benefits and trade-offs between these approaches. Such research efforts will contribute to advancing the field and enabling the development of more efficient and reliable photonic systems for hybrid DRoF and ARoF signal detection in base station configurations.

In summary, the past demonstrations have effectively addressed the issue of baseband signal-to-signal beating interference by shifting the carrierless amplitude/phase (CAP) signal to a higher frequency. However, the proposed single-photodiode signal processing framework offers a more versatile solution that can accommodate various modulation formats. This flexibility is crucial in meeting the growing demand for higher data rates, allowing for the exploration of alternative approaches to cater to evolving communication needs. The proposed signal processing framework provides a practical and adaptable solution that can be readily implemented in analog hardware. This contributes to the simplicity and cost-effectiveness of the system design, making it an attractive option for real-world applications. By enabling the coexistence of hybrid DRoF and ARoF signals using a single photodiode, the proposed approach offers enhanced versatility and facilitates the development of more efficient and flexible photonic systems. As communication requirements continue to evolve, the proposed single-photodiode signal processing framework paves the way for future advancements in optical communication systems, offering a viable solution to meet the increasing demand for higher data rates and improved system performance.

REFERENCES

[1] H. Ji, C. Sun, and W. Shieh, "Spectral efficiency comparison between analog and digital RoF for mobile fronthaul transmission link," *J. Lightw. Technol.*, vol. 38, no. 20, pp. 5617–5623, Oct. 15, 2020, doi: 10.1109/JLT.2020.3003123.

[2] G. Kalfas, C. Vagionas, A. Antonopoulos, E. Kartsakli, A. Mesodiakaki, S. Papaioannou, P. Maniotis, J. S. Vardakas, C. Verikoukis, and N. Pleros, "Next generation fiber-wireless fronthaul for 5G mmWave networks," *IEEE Commun. Mag.*, vol. 57, no. 3, pp. 138–144, Mar. 2019, doi: 10.1109/MCOM.2019.1800266.

[3] L. Zhang, A. Udalcovs, R. Lin, O. Ozolins, X. Pang, L. Gan, R. Schatz, M. Tang, S. Fu, D. Liu, W. Tong, S. Popov, G. Jacobsen, W. Hu, S. Xiao, and J. Chen, "Toward terabit digital radio over fiber systems: Architecture and key technologies," *IEEE Commun. Mag.*, vol. 57, no. 4, pp. 131–137, Apr. 2019, doi: 10.1109/MCOM.2019.1800426.

[4] H. R. D. Filgueiras, E. S. Lima, M. S. B. Cunha, C. H. D. S. Lopes, L. C. De Souza, R. M. Borges, L. A. M. Pereira, T. H. Brandão, T. P. V. Andrade, L. C. Alexandre, G. Neto, A. Linhares, L. L. Mendes, M. A. Romero, and A. Cerqueira, "Wireless and optical convergent access technologies toward 6G," *IEEE Access*, vol. 11, pp. 9232–9259, 2023, doi: 10.1109/ACCESS.2023.3239807.

[5] M. Bakaul, A. Nirmalathas, C. Lim, D. Novak, and R. Waterhouse, "Hybrid multiplexing of multiband optical access technologies towards an integrated DWDM network," *IEEE Photon. Technol. Lett.*, vol. 18, no. 21, pp. 2311–2313, Nov. 1, 2006, doi: 10.1109/LPT.2006.885280.

[6] W.-R. Peng, P.-C. Peng, Y.-T. Hsueh, K.-M. Feng, and S. Chi, "Performance comparisons of external modulated hybrid analog-digital signals in electrical and optical domains," *IEEE Photon. Technol. Lett.*, vol. 17, no. 11, pp. 2496–2498, Nov. 2005, doi: 10.1109/LPT.2005.858152.

[7] C.-T. Lin, J. Chen, P.-C. Peng, C.-F. Peng, W.-R. Peng, B.-S. Chiou, and S. Chi, "Hybrid optical access network integrating fiber-to-the-home and radio-over-fiber systems," *IEEE Photon. Technol. Lett.*, vol. 19, no. 8, pp. 610–612, Apr. 5, 2007, doi: 10.1109/LPT.2007.894326.

[8] P.-T. Shih, C.-T. Lin, W.-J. Jiang, Y.-H. Chen, J. Chen, and S. Chi, "Hybrid access network integrated with wireless multilevel vector and wired baseband signals using frequency doubling and no optical filtering," *IEEE Photon. Technol. Lett.*, vol. 21, no. 13, pp. 857–859, Jul. 1, 2009, doi: 10.1109/LPT.2009.2016574.

[9] S. Shen, J.-H. Yan, P.-C. Peng, C.-W. Hsu, Q. Zhou, S. Liu, S. Yao, R. Zhang, K.-M. Feng, J. Finkelstein, and G.-K. Chang, "Polarization-tracking-free PDM supporting hybrid digital-analog transport for fixed-mobile systems," *IEEE Photon. Technol. Lett.*, vol. 31, no. 1, pp. 54–57, Jan. 1, 2019, doi: 10.1109/LPT.2018.2882766.

[10] S. Yao, Y.-W. Chen, S.-J. Su, Y. Alfadhli, S. Shen, R. Zhang, Q. Zhou, and G.-K. Chang, "Non-orthogonal uplink services through co-transport of D-RoF/A-RoF in mobile fronthaul," *J. Lightw. Technol.*, vol. 38, no. 14, pp. 3637–3643, Jul. 15, 2020, doi: 10.1109/JLT.2020.2980208.

[11] A. Saljoghei, C. Browning, and L. P. Barry, "Spectral shaping for hybrid wired/wireless PON with DC balanced encoding," in *Proc. Microw. Photon. (MWP) 9th Asia–Pacific Microw. Photon. Conf. (APMP) Int. Topical Meeting*, Hokkaido, Japan, Oct. 2014, pp. 307–310, doi: 10.1109/MWP.2014.6994560.

[12] C. Browning, A. Farhang, A. Saljoghei, N. Marchetti, V. Vujicic, L. E. Doyle, and L. P. Barry, "5G wireless and wired convergence in a passive optical network using UF-OFDM and GFDM," in *Proc. IEEE Int. Conf. Commun. Workshops (ICC Workshops)*, Paris, France, May 2017, pp. 386–392, doi: 10.1109/ICCW.2017.7962688.

[13] S. Sarmiento, J. M. D. Mendinueta, J. A. Altabás, S. Spadaro, S. Shinada, H. Furukawa, J. J. V. Olmos, J. A. Lázaro, and N. Wada, "High capacity converged passive optical network and RoF-based 5G+ fronthaul using 4-PAM and NOMA-CAP signals," *J. Lightw. Technol.*, vol. 39, no. 2, pp. 372–380, Jan. 15, 2021, doi: 10.1109/JLT.2020.3028492.

[14] T. S. Rappaport, Y. Xing, O. Kanhere, S. Ju, A. Madanayake, S. Mandal, A. Alkhateeb, and G. C. Trichopoulos, "Wireless communications and applications above 100 GHz: Opportunities and challenges for 6G and beyond," *IEEE Access*, vol. 7, pp. 78729–78757, 2019, doi: 10.1109/ACCESS.2019.2921522.

[15] A. V. Martí, N. Vokic, T. Zemen, and B. Schrenk, "Hybrid CAP/mm-wave OFDM vector modulation for photonic frequency conversion in a single-sideband feeder," in *Proc. Opt. Fiber Commun. Conf. Exhib. (OFC)*, San Diego, CA, USA, Mar. 2022, pp. 1–3.

[16] C.-T. Lin, P. Tsung Shih, J. Chen, P.-C. Peng, S.-P. Dai, W.-J. Jiang, W.-Q. Xue, and S. Chi, "Cost-effective multiservices hybrid access networks with no optical filter at remote nodes," *IEEE Photon. Technol. Lett.*, vol. 20, no. 10, pp. 812–814, May 15, 2008, doi: 10.1109/LPT.2008.921137.

GUO HAO THNG (Member, IEEE) received the B.S. degree in electrical and computer systems engineering and the Ph.D. degree from Monash University Malaysia, in 2017 and 2021, respectively. He is currently a Postdoctoral Researcher with the Zhejiang University-University of Illinois at Urbana-Champaign Institute, Zhejiang University, Haining, Zhejiang, China. His research interests include fiber wireless access networks, and machine learning and signal processing implementation in communication networks.

SAID MIKKI (Member, IEEE) received the Ph.D. degree in electrical engineering from the University of Mississippi, University, MS, USA, in 2008. He is currently an Associate Professor in electrical engineering with the Zhejiang University-University of Illinois at Urbana-Champaign (ZJU-UIUC) Institute, Zhejiang University, Haining, Zhejiang, China, and the Department of Electrical and Computer Engineering, University of Illinois at Urbana-Champaign, Urbana, IL, USA. His current research interests include quantum engineering, electromagnetics, information theory, and artificial intelligence.

• • •